PERGAMON

Neural Networks 14 (2001) 115–131

Neural Networks

www.elsevier.com/locate/neunet

The Bifurcating Neuron Network 1 ☆

G. Lee, N.H. Farhat*

Electrical Engineering Department, University of Pennsylvania, 200 S. 33rd Street, Philadelphia, PA 19104, USA

Received 27 September 2000; accepted 27 September 2000

Abstract

The Bifurcating Neuron (BN), a chaotic integrate-and-fire neuron, is a model of a neuron augmented by coherent modulation from its environment. The BN is mathematically equivalent to the sine-circle map, and this equivalence relationship allowed us to apply the mathematics of one-dimensional maps to the design of BN networks. The study of symmetry in the BN revealed that the BN can be configured to exhibit bistability that is controlled by attractor-merging crisis. Also, the symmetry of the bistability can be controlled by the introduction of a sinusoidal fluctuation to the threshold level of the BN. These two observations led us to the design of the BN Network 1 (BNN-1), a chaotic pulse-coupled neural network exhibiting associative memory. In numerical simulations, the BNN-1 showed a better performance than the continuous-time Hopfield network, as far as the spurious-minima problem is concerned and exhibited many biologically plausible characteristics.

Keywords: Bifurcating neuron; Integrate-and-fire neuron; Time coding; Coherence; Chaos; Attractor-merging crisis; Bifurcating neuron network; Neural network

1. Introduction

There has been a continuing debate on the way information is encoded in neuronal spike trains. The most widely accepted coding scheme is called rate coding, where information is represented by the mean firing rate of a neuron, either in a temporal sense or in a spatial sense (Adrian, 1926; Rieke, Warland, de Ruyter van Steveninck, & Bialek, 1996). Although rate coding has proven to be valid in some neuronal information paths, e.g. in sensory neurons and motor neurons, its validity in other parts of the brain is still questionable. Recent experimental studies are revealing a growing number of new facts beyond the explanation of rate coding and are suggesting the possibility of information coding in the precise timing of neuronal spikes, namely, 'time coding' (Rieke et al., 1996). An especially descriptive example supporting time coding in the brain is provided by O'Keefe (1993), who studied the firing behavior of hippocampal place cells (O'Keefe, 1971) which are located anatomically distant from the sensory and motor cortex. They showed that the firing phases of the place cells with respect to the theta rhythm have a high level of correlation with the animal's location on a linear runway.

Another topic of growing interest among neuroscientists is the role of coherent activities in the brain, especially those in the gamma-band centered around 40 Hz. Some of the early observations of gamma-band oscillatory activities were made in the olfactory bulb and cortex of the rabbit (Freeman & Skarda, 1985), in the olfactory systems of the cat and the rat (Bressler & Freeman, 1980), in a variety of structures of the cat brain (Basar, 1983), in the cat primary visual cortex (Gray & Singer, 1989; Eckhorn et al., 1988), in the monkey visual cortex (Freeman & van Dijk, 1987), and in electroencephalogram (EEG) recordings from the human skull above association and motor areas (Krieger & Dillbeck, 1987). The observation of a synchronous activity in the cat visual cortex by Gray & Singer (1989) has been drawing special attention because, in their experiments, the synchronous activity was stimulus-specific and was observed across cortical regions, e.g. across multiple visual association areas, with a small phase variation. Gray and Singer related their result to the so-called feature-binding hypothesis (Milner, 1974; von der Malsburg, 1981), which states that synchrony provides a means to bind together in time the features that represent a particular stimulus. The searchlight hypothesis of Crick (1984) is another speculation on the role of synchronous activity in relation to the question of consciousness.

☆ A sequel to this paper entitled 'The bifurcating neuron network 2' describing the second type of birfurcating neuron network is in progress.

* Corresponding author.
E-mail address: farhat@ee.upenn.edu (N.H. Farhat).

0893-6080/01/$ - see front matter
PII: S0893-6080(00)00083-6

Nomenclature

$x_i(t)$	the internal potential of neuron i
$\theta_i(t)$	the threshold level of neuron i
$\rho(t)$	the relaxation level of all the neurons in a network
$y_i(t)$	the output of neuron i
$u_i(t)$	the input of neuron i
$t_i(n)$	the n-th firing time of neuron i
$s_i(t)$	the binary state of neuron i
$H(t)$	the pseudo-energy function of a network

Yet another topic of growing interest in neuroscience is the role of chaotic activities in the brain. Different levels of chaotic activities have been observed in many experimental studies of EEG signals, for example, in the simian motor cortex (Rapp, Zimmerman, Albano, Deguzman & Greenbaum, 1985), in the human brain during a sleep cycle (Babloyantz, Nicolis & Salazar, 1985) and during an epileptic seizure (Babloyantz & Destexhe, 1986), and in the olfactory bulb of the rabbit (Freeman & Skarda, 1985; Freeman, 1986). The mounting evidence of chaotic activities in the brain triggered much theoretical reflection on the possible role of chaotic activities in brain functions (Skarda and Freeman, 1987; Yao & Freeman, 1990; Nicolis, 1986, 1991). For instance, Freeman and his coworkers (Freeman & Skarda, 1985) observed in a study of the olfactory system of the rabbit that the nervous activity of the olfactory system switches from a chaotic to a periodic state whenever a familiar odor is detected. This experimental observation stimulated their reflection on the role of chaos in perception processes and led them to postulate that chaos can serve as the ground state of a perception process, i.e. an elevated state that has quick transition routes to many periodic states.[1]

While new questions and findings about the brain are reported every day, these three topics, namely, time coding, coherent activity, and chaotic activity in the brain, are some of the most important topics that can change our understanding of the brain's dynamics at the most fundamental level. It is important to realize, however, that it is not easy to deal with these topics properly in the framework of traditional neural network theory for the following reasons. First, the sigmoidal activation function, which is the neuron model of most traditional neural networks (Hertz, Krough, & Palmer, 1991; Haykin, 1994), is based on the rate-coding hypothesis; the output of a sigmoidal neuron is a continuous real value representing the activity level of a neuron. Second, most traditional neural networks are designed to be dynamically stable and are therefore destined to operate away from a chaotic regime (Hertz et al., 1991; Haykin, 1994). A notable example is the Hopfield network (Hopfield, 1982) where the connection matrix is chosen to be symmetric so that the energy function of the network can always converge to a static attractor. It is even irrelevant to discuss the dynamics of non-recurrent networks, i.e. feed-forward networks, because they do not represent a dynamic system once they are trained. All these considerations lead to the conclusion that the exploration and exploitation of new topics in neuroscience demands a new artificial neural network model.

In fact, the recent trend of artificial neural network theory has seen many new neural models that were inspired by the new findings in neuroscience. Eckhorn, Arndt, and Dike (1990) proposed the linking field model to explain the role of synchronized activity in the visual cortex, and Johnson (Johnson, 1994; Baek & Farhat, 1998) applied the model to a problem of pattern recognition. Hopfield (1995) also proposed a pattern recognition mechanism benefiting from the synchronized activity of pulse-coupled neurons. Freeman and van Dijk (1985) implemented a model neural network that can explain the behavior of the olfactory bulb of the rabbit, and stimulated the design of many new neural networks that utilize chaotic model neurons. Aihara et al. (1990) modified the Hopfield network and developed a chaotic neural network consisting of neurons capable of exhibiting chaotic behaviors induced by self-coupling. Nozawa (1992) derived a chaotic neural network by using an Euler discretization on the Hopfield model. Wang and Smith (1998) developed another type of network by varying the time step of an Euler discretized Hopfield network. Many of these new chaotic networks can be understood from the viewpoint of the coupled map lattice (CML) introduced by Kaneko (1992, 1993). In this respect, some recent studies on CML (Holden, Tucker, Zhang, & Poole, 1992) and its variations (Farhat & Hernandez, 1995) can also be counted toward the effort to develop chaotic neural networks. More examples of a new network design include Natschlaeger and Ruf (1998); Maass and Natschlaeger (1998). It is important to note, however, that few of these new network designs address time coding, coherent activity, and chaotic activity, all together. In reality these three issues are closely related and often arise concurrently playing their respective roles. In our study, we focused on the new possibilities that can arise where these three issues converge.

An obvious requirement for an artificial neural network based on time coding is a 'time-coding capable' model neuron: a neuron that can deal with information encoded in a spike train. One of the simplest examples of such a model is the integrate-and-fire neuron (Knight, 1972), where a neuron is approximated by a leaky integrator of a postsynaptic current. At the other extreme are compartment models of a neuron (Segev, Fleshman, & Burke, 1989), where neuronal spatial structure, as well as the dynamics of various ionic channels, are taken into consideration to

[1] This concept is in fact very reminiscent of the concept of 'controlling chaos' (Ott, Grebogi, & Yorke, 1990) in nonlinear control theory where a strange attractor is regarded as a set of an infinite number of unstable periodic orbits (Grebogi, Ott, & Yorke, 1987), one of which can be stabilized by the proper control mechanism.

reproduce the actual behavior of a neuron as closely as possible. Choosing a model neuron of the proper complexity is not an easy task because the nature of the approximation implied by a certain model is often unclear until the model is tested in a network. An obvious minimum requirement would be the ability to produce a spike train output, where information is represented not by the amplitude but by the time of a spike, and the ability to respond sensitively to the timing of incoming spikes. Since both of the two extreme examples, i.e. the integrate-and-fire neuron and the compartment-model-based neurons, appear to satisfy the requirement, it is a wise strategy to try first the simplest, and therefore we chose the integrate-and-fire neuron as the starting point of our neuronal modeling.

The next issue is how to utilize coherence in our model neuron or model network. Although we are using the expression 'utilizing coherence', this is not well defined and demands further clarification. It is easy to design an integrate-and-fire neuron network that autonomously evolves into a synchronized, or coherent, state (Mirollo & Strogatz, 1990; Bottani, 1995; Abbott & van Vreeswijk, 1993). The question that remains, however, is what can be done with it. The problem is that the role coherence plays in the operations of the network has not been identified clearly. Although the role of coherence is still the focus of debate, it is necessary to define a role of coherence that can guide our network design. The one that we chose over other possibilities states that a coherent activity in an integrate-and-fire neuron network can provide a time reference. This role may sound excessively general or even trivial, but it is certainly essential. In the absence of a time reference, the information that time coding can carry would be severely limited. The aforementioned O'Keefe and Recce (1993) experiment is a good example for such a role of coherence (the theta rhythm). The fact that rate coding is common in sensory or motor neurons is also consistent with such a role of coherence: rate coding must be the only choice when a common time reference extending throughout the nervous system is not available. If the role of coherence in biological systems is to provide a time reference, we do not need to complicate the design of our network by adding a mechanism to produce coherence; we can provide a time reference from outside.

The final issue is how to utilize chaos. A chaotic activity may arise either from a neuron itself or from the interaction of non-chaotic neurons. An example of the latter case is given in Sompolinsky and Crisanti (1988), where a mean-field analysis is used to show that a network of sigmoidal neurons with random, non-symmetric coupling weights can be put into a chaotic operating regime when the overall coupling strength exceeds a certain limit. In fact, this is not an exceptional case because any nonlinear dynamic system consisting of at least three state variables is known to have the potential of exhibiting chaos (Hilborn, 1994). In this respect, the next example can be the Lorentz system (Hilborn, 1994), which is a classical example of three-variable dynamic systems capable of exhibiting chaos, because it may be regarded as a network of non-chaotic neurons, where each integrator represents a neuron. These two examples suggest that the possibility of a chaotic network out of non-chaotic elements is plentiful. However, we decided to follow the other option, a network of chaotic neurons, for the following reason. Chaotic activity will be more useful in the 'ready-state' of a network where the network is ready to respond to an external stimulus. In other words, we have the following scenario in mind: a stimulus known to a network causes the interconnections in the network to interfere constructively, and thereby suppress the initial chaotic activity in the network. This scenario assumes that the network is in a chaotic state before strong interaction among the neurons is established. In short, this scenario requires chaotic neurons. This scenario is in fact inspired by the aforementioned experimental observation of Freeman & Skarda (1985) and also by some recent studies that show that the behavior of individual neurons in isolation is more irregular than that of neurons in a network (Rabinovitch & Abarbanel, 1998).

Our model neuron is derived from the integrate-and-fire neuron model for the reason stated above. The behavior of an integrate-and-fire neuron under a constant feeding is simple: it repeats a regular cycle of charging and discharging. This simple picture of an integrate-and-fire neuron is of course due to an unrealistic assumption about the environment surrounding the neuron. A neuron in a biological neural network receives inputs from many different parts of the brain and is also subject to noise from inside and outside. Also, the same input can have different effects depending on the nature and the position of the synapse. Consideration of every detail of the interaction of a neuron with its environment would be impractical, so we made the following rather simplistic assumptions about the artificial environment surrounding an integrate-and-fire neuron. First, the environment provides a persistent incoherent input to the neuron, which helps the neuron keep active at an optimal operating point. Second, the environment also provides a persistent coherent input to the neuron, which is common to all the neurons in the same network and serves as a time reference.

It is possible to design a network such that it can provide itself with such incoherent and coherent inputs. For instance, some extra diffuse connections can be added between model neurons so that the neurons can feed each other with an incoherent input. Also, a part of the network can be used to build a pace maker that can provide a coherent input to other parts of the network. However, any attempt to model a biological neural network cannot avoid an approximation at some part or level of modeling. Here, we are approximating the mechanisms that are responsible for the incoherent and the coherent input by simply calling them 'the environment'. This way, we can focus on what happens when a time-coding-aware model network is subjected to such background activities. In this respect, our neuron model does not represent a neuron as it is, but a neuron augmented by incoherent activities and coherent

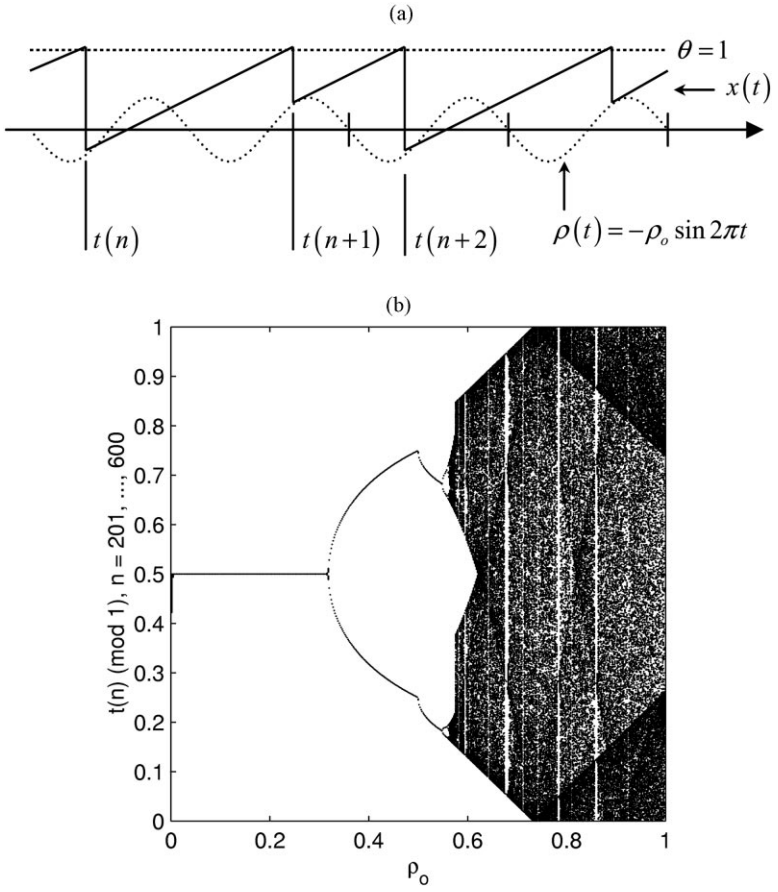

Fig. 1. The Bifurcating Neuron: a, the behavior of the BN in the absence of an input: it keeps firing due to an incoherent source while the relaxation level is oscillating due to a coherent source; b, firing times of the BN with respect of a modulus of 1, which is the period of the sinusoidal oscillation of the relaxation level.

activities in its environment. This is akin to the concept of an electron with an effective mass in solid state physics: an electron with an effective mass is not a model of an electron standing alone in the vacuum, but a model of an electron augmented by the influence of the atoms in the lattice surrounding it.

The following set of equations defines our model neuron:

$$\frac{\mathrm{d}x}{\mathrm{d}t} = c \tag{1}$$

$$\rho(t) = -\rho_0 \sin 2\pi f t \tag{2}$$

$$\theta(t) = 1 - \delta(t) \tag{3}$$

where x is the internal potential of the neuron, and c, ρ_0 and f are positive constants. Eq. (1) describes the constant buildup of the internal potential due to the constant feed by an incoherent source. Eq. (2) describes the oscillating relaxation level due to a sinusoidal stimulation by a coherent source. Eq. (3) describes the perturbation $\delta(t)$ in the threshold level induced by an input from the presynaptic neuron. Fig. 1a depicts the behavior of our model neuron in the absence of an input (i.e. $\delta(t) = 0$): it keeps firing due to an incoherent source while the relaxation level is oscillating due to a coherent source. An important fact to emphasize again here is that the coherent source serves as a time reference to the neuron. This fact is clearly demonstrated in Fig. 1b, that shows the firing times of the neuron with respect to a modulus of 1, which is the period of the sinusoidal oscillation of the relaxation level. Although the firing of the neuron here is not always phase-locked to the sinusoidal oscillation, the firing time exhibits a clear structure when it is represented relative to the sinusoidal oscillation. In addition to providing a time reference, the coherent source turns the neuron into a chaotic neuron. This fact is also demonstrated in Fig. 1b, where one can see that the firing pattern is bifurcating until it becomes chaotic as the amplitude of the sinusoidal oscillation increases. This dynamic behavior of a neuron subjected to an oscillatory input has been a subject of interest among many researchers (Holden & Ramadan, 1981; Hayashi, Ishizuka, Ohta, & Hirakawa, 1982; Aihara & Matsumoto, 1986), and a detailed treatment of the same theme, applied to an integrate-and-fire model, appears in Farhat and Eldefrawy, 1991, 1992. Farhat and Eldefrawy discovered that an integrate-and-fire model neuron can operate in dynamically distinct modes of operation

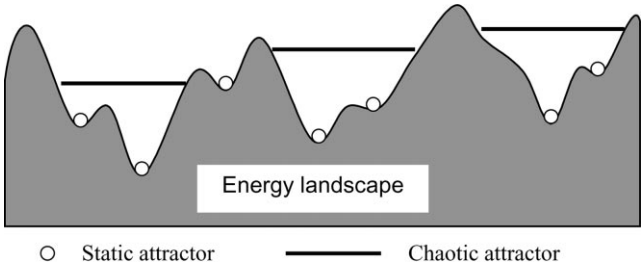

Fig. 2. A conceptual illustration of fixed point attractors and chaotic attractors in an imaginary energy landscape.

depending on the amplitude and frequency of the applied oscillatory input, and showed that such a model neuron is mathematically equivalent of the sine-circle map (Hilborn, 1994). Since this equivalence relationship plays a central role in the development of our networks, we call our neuron model a Bifurcating Neuron (BF), which is the name that Farhat and Eldefrawy used to emphasize the bifurcating behavior of an integrate-and-fire neuron under a sinusoidal modulation.[2]

We have been exploring the potential of various types of BN networks. In this paper, we introduce a BN network that we call the Bifurcating Neuron Network 1 (BNN-1). The BNN-1 is a binary associative memory exploiting the bistability of the BN which appears when the average firing frequency of a BN is twice that of the relaxation level oscillation. The two chaotic attractors which account for the bistability are subject to attractor-merging crisis (Grebogi, Ott, & Yorke, 1987); merging or separation of the two attractors is critically dependent on the amplitude of the relaxation level oscillation. Near the point of crisis, a sinusoidal perturbation in the threshold level induced by an incoming spike train can bias the bistability, thereby inducing a binary transition. The result is a binary associative memory where a memory is represented by a chaotic attractor. Fig. 2 is a conceptual illustration of fixed point attractors and chaotic attractors in an imaginary energy landscape. A chaotic attractor lives in a state space occupying a certain non-zero volume. At first glance, this may seem disadvantageous because a state space of the same size will be able to accommodate a smaller number of chaotic attractors than fixed point attractors. However, this is more an advantage than a disadvantage because it endows a network with robustness. An associative memory utilizing chaotic attractors is less subject to the spurious minima problem, which often arises in networks based on fixed point attractors. Another advantage of a chaotic-attractor-based memory, as implied in Fig. 2, is that the network never dissipates to the ground level, but maintains its activity even after it settles on a chaotic attractor. This means that the network will be more ready to respond to an external stimulus. As will be shown in the comparison with the continuous-time Hopfield network, the BNN-1 is indeed less susceptible to the spurious minima problem. If the initial state of the network does not fall in one of the basins of attractions of the patterns embedded in it, it never converges to a stable pattern, implying 'I don't know'. Otherwise, it would almost always converge to one of the embedded patterns. Associative memory networks that overcome the limitations of the Hopfield network have been proposed by many authors (Aihara & Takabe, 1990; Nozawa, 1992; Wang & Smith, 1998) as mentioned earlier. However, the BNN-1 is one of the rare examples of integrate-and-fire neuron networks that use chaotic attractors to enhance associative memory performance.

In Section 2, starting with the study of the symmetry in the sine-circle map, we will investigate the bistability and the attractor-merging crisis in the BN. In Section 3, we will be in search of a control parameter to control the bistability of the BN, and, in Section 4, we will arrive at an efficient pulse-coupling scheme to be used in the BNN-1. In Section 5, we will define an associative memory test and give a test result for the continuous-time Hopfield network which can be used as a benchmark to assess the performance of the BNN-1. In Section 6, we will complete the mathematical definition of the BNN-1 and build an associative memory out of it. We will examine closely the recall process of the BNN-1 and compare it with that of the Hopfield network. In the concluding section, we will discuss the unique dynamical characteristics of the BNN-1 that distinguish it from other types of neural network.

2. Bistability and attractor-merging crisis of the BN

We started our search for the bistability and the attractor-merging crisis of the BN with a study of symmetry in the sine-circle map (recall that the BN is mathematically equivalent to the sine-circle map) since attractor-merging crisis is the interaction between two symmetric attractors. It is known that bimodal, symmetric one-dimensional maps, such as the cubic map and the sine map, exhibit attractor-merging crisis (Grebogi, Ott, & Yorke, 1987). The symmetry that gives rise to the symmetric attractors of such maps is an inversion symmetry. For instance, if we change every occurrence of x in the recursion of the sine map,

$$x(n+1) = \eta \sin \pi x(n), \tag{4}$$

to $-x$, we see that the recursion is unchanged. Then we ask, can we also find such symmetry in the sine-circle map? To answer this question, let us take a look at the recursion of the sine-circle map:

$$x(n+1) = x(n) + \Omega + \frac{K}{2\pi} \sin 2\pi x(n) \qquad (\text{mod } 1). \tag{5}$$

Apparently, we can see here no such inversion symmetry as in the case of the sine map. However, we can see a different type of symmetry: a translation symmetry due to the

[2] The term Bifurcating Neuron was introduced independently by Farhat (Farhat & Eldefrawy, 1991) and Holden (Holden, Hyde, Muhamad, & Zhang, 1992).

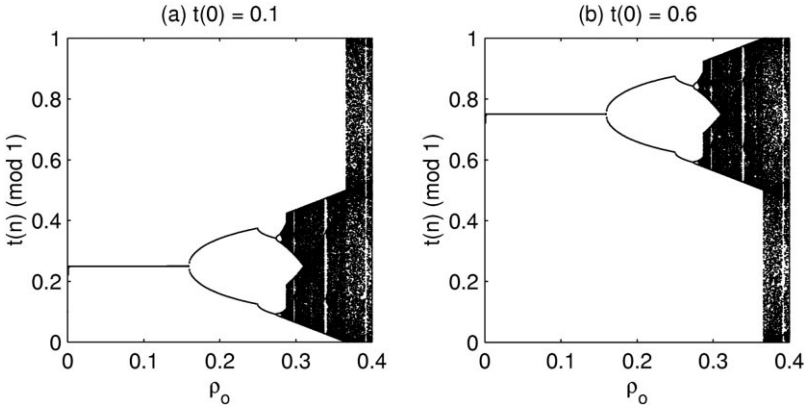

Fig. 3. The bifurcation diagrams of the BN for $f = 2$, which show the firing behavior of the BN as the birfurcation parameter ρ_o changes. These two different bifurcation diagrams are the results of the following two different initial conditions: a, $t(0) = 0.1$ and b, $t(0) = 0.6$.

periodicity of the sine function. If we change every occurrence of x in Eq. (5) to $x + 1$, the equation remains unchanged.

Now, we can restate this result in terms of the BN. In the absence of an input, the set of equations defining the BN, Eqs. (1)– (3), becomes

$$\frac{dx}{dt} = 1, \qquad \theta = 1, \qquad \rho(t) = -\rho_0 \sin 2\pi f t, \tag{6}$$

where, without loss of generality, we assumed that the constant buildup rate c is 1. The recursion that accounts for the firing time of the BN is given by

$$t(n+1) = t(n) + 1 + \rho_0 \sin 2\pi f t(n). \tag{7}$$

As in Eq. (5), we can also see here a translational symmetry due to the periodicity of the sine function. If we change every occurrence of t in Eq. (7) to $t + 1/f$, the equation remains unchanged.

Fig. 3 shows the bifurcation diagrams of the map defined by Eq. (7) when $f = 2$. As in the case of the sine-circle map, the vertical axis represents $t(n)$ (mod 1), i.e. the firing time of the BN with respect to a modulus of 1, where 1 is the firing period of the BN in the absence of the relaxation level oscillation. As we expected, we can see two symmetric attractors which divide the entire state space [0, 1), in the sense of a modulus of 1, into two equal intervals. Except that the onset of the two attractors is not initiated by a pitchfork bifurcation, the overall pattern of bifurcation is very similar to that of the sine map. Again, as in the case of the sine map, there is an unstable fixed point at $t = 0.5$, which is separating the two attractors. When the attractors expand until it touches the unstable fixed point, they undergo a crisis and collapse into a single fully chaotic attractor.

The value of the bifurcation parameter ρ_0 at which the attractor-merging crisis takes place will be called a crisis point point ρ_0^c. A simple graphical method showed that its value is the solution of the following implicit equation:

$$\sqrt{\rho_0^{c^2} - \frac{1}{16\pi^2}} + \frac{1}{4\pi} \arccos\left(-\frac{1}{4\pi\rho_0^c}\right) - \frac{1}{2} = 0. \tag{8}$$

It is not possible to obtain an exact analytic solution to this equation; a numerical method gave an approximate solution of $\rho \approx 3.633$.

One last thing to point out before ending this section is that the bistability implied by the two symmetric attractors is, in fact, a special case of the multi-stability of the BN. When $f = 3$, the BN has three symmetric attractors and exhibits tri-stability. The BN will come to have a multi-stability with a larger number of symmetric attractors, as f is increased further. Such a multi-stability of the BN may be worth further investigation. At this point, however, we do not have any concrete idea of how to utilize such multi-stability and have therefore concentrated on the case of $f = 2$.

3. Controlling bistability of the BN

Now that the BN is shown to have bistability and exhibit attractor-merging crisis, the next question is how to couple them together to form a network that can perform a meaningful function. If the bistability of the BN encodes binary information, a natural role of the desired coupling scheme is to control the bistability. In short, we need to find out a mechanism to break symmetry in the bistability of the BN.

Among other possible ways to break the symmetry, the following method would be one of the simplest, yet biologically plausible, ones. In Eq. (6), which led to Fig. 9, the threshold level θ is constant. In the case of biological neurons, however, the threshold level, as well as the internal potential, is affected by postsynaptic potentials. One way to break the symmetry of the bistability is to introduce to the threshold level a sinusoidal oscillation of half the frequency

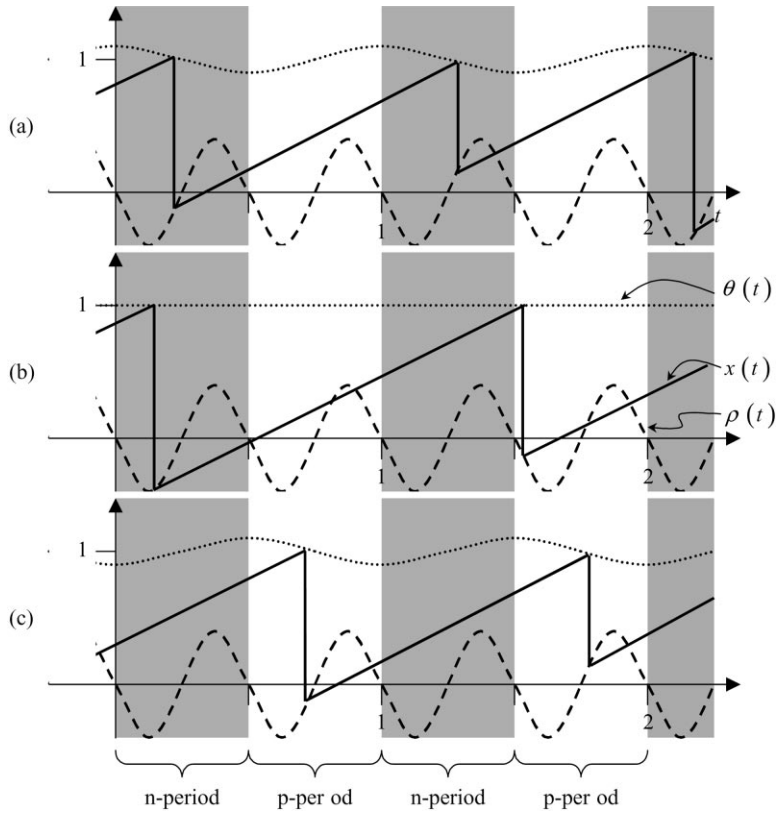

Fig. 4. The expected firing behavior of the BN for three different amplitudes of the threshold oscillation: a, $\varepsilon = -0.1$; b, $\varepsilon = 0$; and c, $\varepsilon = 0.1$.

of the relaxation level oscillation:

$$\theta(t) = 1 + \epsilon\cos 2\pi t. \tag{9}$$

Fig. 4 shows the expected behavior of the BN for three different amplitudes of the threshold oscillation: $\varepsilon = -0.1$, 0 and 0.1. In all three cases, it is assumed that the driving amplitude ρ_0 is a little larger than the crisis point $\rho_0^c \approx 3.633$. This means that, when $\varepsilon = 0$, the BN will be in a fully chaotic state and can fire at any point in the state space [0, 1) (in the sense of a modulus of 1). When $e = -0.1$, the symmetry that gives rise to the two symmetric chaotic attractors of the BN, which were shown in Fig. 3, is now broken. As a result, the first half of the state space becomes more stable than the second half, thereby the BN is more likely to fire in the first half than in the second half. The situation is reversed when the sign of the modulation amplitude ε is reversed. The bottom line is that the translation symmetry of the BN is broken by the sinusoidal oscillation of the threshold level of the form given by Eq. (9). In other words, the preference of the BN over the two symmetric attractors can be controlled by the sign of ε.

For the further discussion of the bistability of the BN, we need to define the binary state of the BN. The BN is considered to be in the negative state if it is firing in the first half of the state space [0,1) with respect to a modulus 1. Likewise, it is considered to be in the positive state if it is firing in the second half. The definition of the binary state at an arbitrary time t can become ambiguous when the BN is in a fully chaotic state as in the case of Fig. 4b. The following definition of the binary state variable of the BN will help clear such an ambiguity:

$$s(t) = \begin{cases} -1 & t(n) \in [0\ 0.5) \quad (\text{mod } 1) \\ 1 & t(n) \in [0.5\ 1) \quad (\text{mod } 1) \end{cases} \tag{10}$$

where $t(n)$ is the last firing time of the BN. For ease of illustration, we will call the first half and the second half of the state space as *n-period* and *p-period*, respectively, hereafter. Since the two periods are defined with respect to a modulus 1, they will divide the time axis into an alternating series of n-periods and p-periods, as illustrated in Fig. 4.

Fig. 5 shows bifurcation diagrams of the BN with the amplitude of the threshold oscillation ε being the bifurcation parameter. They show the behavior of the firing time ($t(n)$ (mod 1)) of the BN as the amplitude ε changes. The firing times of the BN are confined to either half of the state space when the magnitude of ε is larger than a certain threshold, whereas the firing times spread over the entire state space [0, 1) otherwise. The overall shape of the bifurcation diagrams tends to recall the sigmoidal curve, which is a popular model of the neuron response. However, a pronounced difference is observed in the intermediate region of the bifurcation parameter: the response of the BN is not static but dynamic. It is always ready to hop between the two chaotic attractors. Such an indeterminate

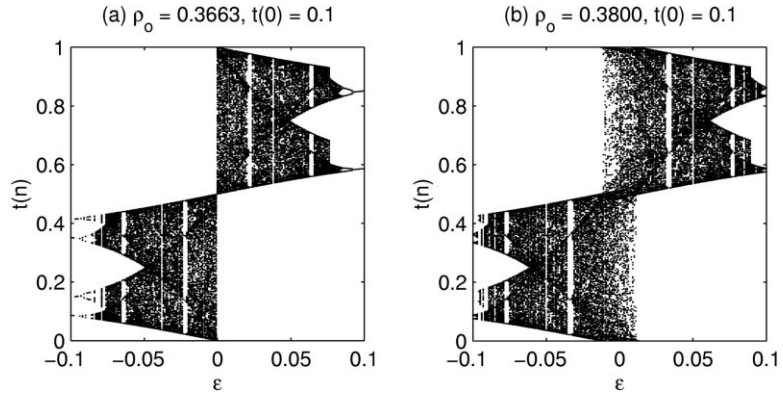

Fig. 5. The bifurcation diagrams of the BN, which show the firing behavior of the BN as the birfurcation parameter ε changes, for the following two cases: a, $\rho_0 = 0.3663 \approx \rho_0^c$ and b, $\rho_0 = 0.38 > \rho_0^c$.

behavior becomes maximized when the bifurcation parameter ε is near zero.

4. Pulse-coupling via harmonic oscillator

Now we are at the stage of completing our formulation of the coupling scheme for the BNN-1. We have seen that the symmetry of the BN can be broken by an introduction of threshold level oscillation and its bistability can be controlled by the oscillation amplitude. However, the input that a BN receives from the presynaptic BNs is in the form of a spike train. Apparently, we need to provide a linkage between the spike train and the threshold level oscillation. We can come put with an immediate solution when we note that the sinusoidal function is the impulse response of the harmonic oscillator. We propose that the threshold level of the BN be modeled by the harmonic oscillator that is subject to an impulsive input:

$$\frac{d^2\theta}{dt^2} + \gamma\frac{d\theta}{dt} + \omega_0^2\theta(t) - \omega_0^2 = u(t) \tag{11}$$

where $\omega_0 = 2\pi/\sqrt{1 - 1/4Q^2}$, $\gamma = \omega_0/Q$ and Q is the Q-factor of the harmonic oscillator. The role of the constant term $-\omega_0^2$ on the left side of the equation is to shift the equilibrium point of the oscillation from 0 to 1, and it cannot affect the dynamics of the system in any way. The spiky input $u(t)$ from the presynaptic BNs is driving the harmonic oscillator. Note that the oscillator parameters are carefully chosen so that the oscillation frequency is 1 when the oscillator is under-damped. It is expected that the oscillator will respond to the periodicity of period 1 in the incoming spike train. This also means that, if the spike intervals are irregular, the response of the oscillator will be minimal. As an aside, we emphasize that the proposed coupling scheme does not require any complicated arithmetics which is difficult to implement in a circuit. The BNs in the network emit spikes, and the spikes are delivered to the target BNs as they are. The only additional component we need is a harmonic oscillator, which has a natural counterpart such as an RLC filter or an active filter.

At this point, one may raise the following questions. First, how can the presynaptic BNs maintain the period and the phase of its output spike train in order to be effective on the target BN? The answer lies in the common driving signal that modulates the relaxation level of all the BNs in the network. All the BNs will fire roughly in phase after they settle down to a steady state. Second, does the harmonic oscillator have any biological relevance? Our answer to this question cannot be very meaningful because the BN, our neuron model, is not a detailed model of the biological neuron, that involves complicated interactions of the various ionic channels. Nevertheless, if the biological justification is still desired, we are ready to explain. One of the most simple but widely used linear models of dendritic processing is the alpha function (McKenna, Davis, & Zornetzer, 1992). Although the theory that leads to the alpha function does not involve any inductance in the dendrite model, the alpha function itself is a solution of the second-order linear differential equation. In fact, it is a solution of Eq. (11) when the Q-factor is chosen such that the oscillator is critically damped ($Q = 1/2$). In this case, ω_0 in Eq. (11) corresponds the exponent of the alpha function.

The only gap that is left for us to fill regards the Q-factor. As we will see later, we require it to be larger than 1/2, i.e. we need an under-damped harmonic oscillator. At first glance, the gap seems to be too wide to fill because an under-damped harmonic oscillator needs an inductance, and an inductance in the neuron membrane sounds rather unrealistic. On second thought, however, we see some light in the voltage-dependent conductance of the neuron membrane: if a neuron membrane experiences a voltage-dependent conductance change, its equivalent circuit will behave as if it contains an inductance. Indeed, there are many theoretical and experimental findings that support 'phenomenological inductance' in the neuron membrane. Hodgkin and Huxley (1952) model of the squid giant axon also reflected this inductive property. In their model, the membrane potential behaves in a similar way to the

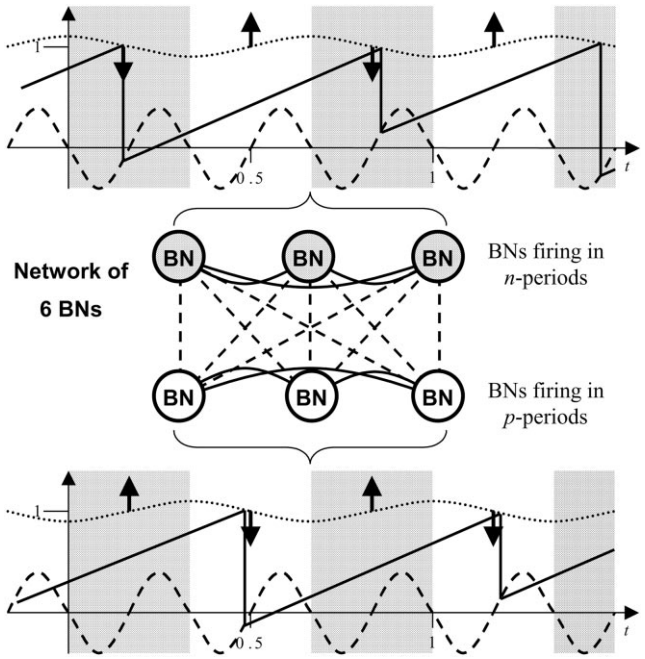

Fig. 6. A small example network to illustrate the operation of the proposed pulse-coupling scheme.

output of an RLC circuit; the membrane potential, according to their model, exhibits damped oscillation as it returns to the resting value. A good review on phenomenological inductance in the neuron membrane is found in Wheeler (1998). We can at least say that the harmonic oscillator as a model of the threshold level of the neuron is not entirely artificial.

Fig. 6 shows a small example network to illustrate the operation of the proposed pulse-coupling scheme. The solid lines among BNs represent excitatory connections, while the dashed lines represent inhibitory connections. Suppose that the BNs are divided into two groups: three BNs firing in the n-period and the other three BNs firing in the p-period. The first temporal plot shows the expected state evolution of one of the BNs in the first group. The thick downward arrows represent the spike input from the BNs in the same group, while the thick upward arrows represent the spike input from the BNs in the other group. These inputs together will induce sinusoidal oscillation of the threshold level, as shown in the plot, and the oscillation is in such a phase as to reinforce the firing of the BN in the n-periods. The second temporal plot shows the expected state evolution of a BN in the second group. The situation is similar to that of the first plot, but this time, the resulting sinusoidal threshold level is in such phase as to reinforce the firing of the BN in the p-periods. In conclusion, the pulse-coupling scheme seems to maintain the clustering of a network into such two groups. Of course, as one can see in the figure, the two groups are determined by the configuration of the excitatory and inhibitory connections.

5. An associative memory test

Before we give the complete definition of the BNN-1 in the next section, we will define an associative memory test in this section and use it to assess the performance of the Hopfield network against which that of the BNN-1 will be evaluated.

The associative memory test uses the six binary training patterns shown in Fig. 7, where a black color represents -1, while a white color represents 1. We will use the symbol $\mathscr{P}_k$ to denote the binary patterns:

$$\mathscr{P}_k = \left\{\xi_i^k\right\} \tag{12}$$

where $k = 1, 2, \ldots, K$ is the index to the patterns and ξ_i^k represents the binary pixels that can be -1 or 1. Each pattern contains 64 binary pixels, i.e. $i = 1, 2, \ldots, I$ and $I = 64$.

After the training patterns are embedded in the weight matrix of the network under test, the network will be subjected to 1000 random trials. In each trial, the network will be started with a random initial state and will then be allowed a certain amount of time to converge to a stable pattern. *If the network fails to converge to a stable pattern, the trial will be repeated with a new random initial condition until the network succeeds in converging to a stable pattern.* Such a retrial will never be necessary for the Hopfield network, since it is based on the gradient descent dynamics and, therefore, is guaranteed to converge to a fixed point. On the other hand, if the network is not based on the gradient descent dynamics, as is the case in the sine map networks, it may or may not converge to a fixed point. For such a network, a failure to converge should not be counted towards

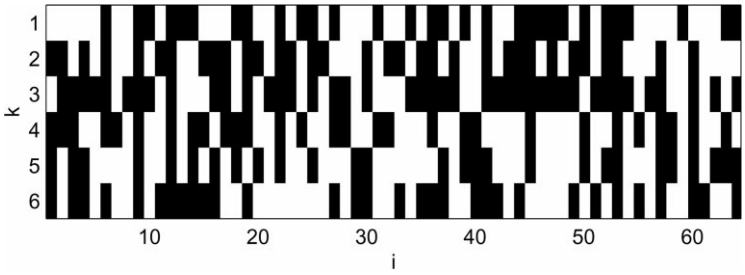

Fig. 7. The six random binary training patterns that will be used in the associative memory test: black represents -1 and white represents 1.

Table 1
The recall statistics of the Hopfield network. The table shows the respective numbers of convergences to the training patterns and the reversed patterns for several different choices of the parameter β

β	$\mathscr{P}_1$	$\overline{\mathscr{P}}_1$	$\mathscr{P}_2$	$\overline{\mathscr{P}}_2$	$\mathscr{P}_3$	$\overline{\mathscr{P}}_3$	$\mathscr{P}_4$	$\overline{\mathscr{P}}_4$	$\mathscr{P}_5$	$\overline{\mathscr{P}}_5$	$\mathscr{P}_6$	$\overline{\mathscr{P}}_6$	Total
0.20	50	56	61	57	69	77	28	36	30	32	43	53	592
0.10	51	53	73	67	63	75	88	85	27	20	42	39	683
0.05	38	37	71	57	61	70	0	0	0	0	32	33	399
0.03	21	16	60	48	54	48	0	0	0	0	5	8	260

a 'false recall', since it indicates that the given initial pattern is unknown or ambiguous to the network. In fact, this type of response is biologically plausible since it more resembles that of the biological neural network than the compulsive convergence behavior of the gradient-descent networks. A striking experimental evidence that supports this point of view is found in Freeman and Skarda (1985)) and Skarda and Freeman (1987).

The stable pattern after the network converges will be compared with the training patterns and the reversed training patterns by evaluating the following metric:

$$d_k = \frac{1}{I}\sum_{i=1}^{I} s_i \xi_i^k \tag{13}$$

where s_i is the binary representation of the final state of the network; its definition will vary depending on the type of network. The metric can take values from -1 to 1; $d_k = 1$ indicates the network has converged to the pattern $\mathscr{P}_k$ and $d_k = -1$ indicates the network has converged to the reversed pattern $\overline{\mathscr{P}}_k$. The metric, taking a value in between, indicates a 'false recall', i.e. the network converges to a false pattern that is not among the training patterns or their reversed versions. During the 1000 trials, the respective numbers of convergences to the training patterns and the reversed patterns will be counted and tabulated as shown in Table 1.

5.1. The continuous-time Hopfield network

There are two different versions of the Hopfield network: discrete time version and continuous time version (Hertz, Krough, & Palmer, 1991). We tested both versions and decided to use the continuous time version for our comparison purposes since the recall quality of the discrete time version was far below that of the continuous time version. In the following discussion, we will use the name Hopfield network to specifically refer to the continuous time version.

The Hopfield network is defined by the following set of differential equations (Hertz, Krough, & Palmer, 1991):

$$\tau_i \frac{\mathrm{d}x_i}{\mathrm{d}t} = -x_i(t) + g\left(\sum_j^I w_{ij} x_j(t)\right) \tag{14}$$

where $x_i(t)$ is the state or activation of neuron i and τ_i is the time constant of neuron i. We will choose it to be identical for all neurons in the network. In this case, it can be absorbed in the time variable by a suitable normalization, and it can therefore be set to 1 without loss of generality. The weight matrix w_{ij} is determined by the Hebbian rule (Hebb, 1949):

$$w_{ij} = \sum_{k=1}^{K} \xi_i^k \xi_j^k \tag{15}$$

The function $g(u)$ represents the graded response of the neuron and has a saturation nonlinearity. It is usually chosen to be $\tanh(\beta u)$. In this case, the parameter β acts like the annealing parameter or the reciprocal of the temperature parameter of the Boltzman machine. Therefore, the recall process of the Hopfield network is appreciably affected by the parameter β. When β is large, the network is effectively operating at a low temperature and converges more rapidly, but is more likely to be trapped in a spurious minimum. When β is small, the situation is reversed. Because the state variable x_i does not always saturate after convergence, especially when β is small, it is necessary to define a binary state variable:

$$s_i(t) = \mathrm{sgn}(x_i(t)). \tag{16}$$

The associative memory test was repeated several times for different values of the parameter β, since the recall quality of the Hopfield network is highly dependent on the choice of β. The test results are shown in Table 1. It shows the respective numbers of convergences to the training patterns and the reversed patterns for several different choices of the parameter β. The best result was obtained when $\beta = 0.1$: in this case, the network could successfully recall a correct pattern in about 68% of the 1000 trials. In the rest of the trials, the Hopfield network was trapped in a spurious minimum and resulted in a false recall.

The time evolution of the Hopfield network in one of the successful recall trials is shown in Fig. 8 (the symbol r.s. in the figure represents the random number seed that was used to determine the random initial condition of the network in the trial). The top plot shows the transition of the binary state variables $s_i(t)$ and the middle plot shows the trajectories of all the state variables $x_i(t)$. The bottom plot shows the time evolution of the pseudo energy function, which is defined as follows:

$$H(t) = -\sum_{i=1}^{I}\sum_{j=1}^{I} w_{ij} s_i(t) s_j(t). \tag{17}$$

We call this the 'pseudo' energy function because it is not the Lyapunov function of the Hopfield network, but is simply a measure of conflict in the binary Hebbian network. Apparently, it is at a local minimum when $s_i(t)$ is one of the training patterns embedded in the weight matrix w_{ij}. We decided to use this pseudo energy function because it can also be used for the BNN-1 that will be compared with the Hopfield network in the following sections.

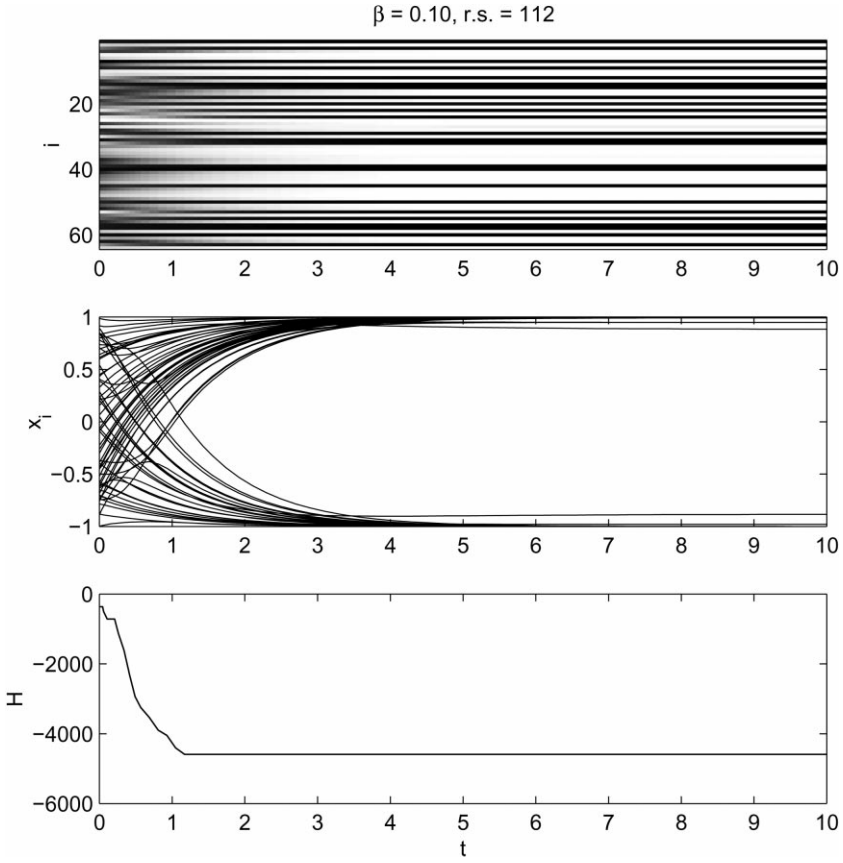

Fig. 8. The time evolution of the Hopfield network in one of the successful recall trials: (top) the transition pattern of the binary state variables $s_i(t)$; (middle) the trajectories of all state variables $x_i(t)$; and (bottom) the trend of the pseudo energy function H(t) during the recall process.

6. The bifurcating neuron network 1

Consider a network of I BNs that is governed by the following equation:

$$\frac{dx_i}{dt} = 1, \qquad i = 1, 2, \ldots, I. \tag{18}$$

The state variable $x_i(t)$ increases linearly until it reaches the threshold level $\theta_i(t)$ and then drops down to the relaxation level $\rho_i(t)$. All the BNs in the network have the same relaxation level:

$$\rho_i(t) = -\rho_0 \sin 4\pi t. \tag{19}$$

A spike train out of a BN can be represented by a series of Dirac-delta functions

$$y_i(t) = \sum_{n=1}^{\infty} \delta(t - t_i(n)) \tag{20}$$

where $t_i(n)$ is the n-th firing time of BN i. The weighed sum of spike trains from the presynaptic BNs induces an oscillation in the threshold level of the BNs. Eq. (11) now becomes:

$$\frac{d^2\theta_i}{dt^2} + \gamma\frac{d\theta_i}{dt} + \omega_0^2[\theta_i(t) - 1] = -d\sum_{j=1}^{I} w_{ij} y_j(t) \tag{21}$$

where d is a coefficient that controls the overall coupling strength among the BNs. In the under-damped case, the impulse response of the threshold level is of the form $e^{-\gamma/2}\sin\omega_r t$, where $\omega_r = \sqrt{\omega_0^2 - \gamma^2/4}$. Since we want the threshold level oscillation to be most sensitive to an external stimulus of the unit frequency, it is required that $\omega_0 = 2\pi/\sqrt{1 - 1/4Q^2}$ and $\gamma = \omega_0/Q$. The coupling weights w_{ij} are determined by the Hebbian rule (Hebb, 1949):

$$w_{ij} = \sum_{k=1}^{K} \xi_i^k \xi_j^k \tag{22}$$

where $\mathscr{P}_k \equiv \{\xi_i^k\}$, $k = 1, 2, \ldots, K$, are the K training patterns shown in Fig. 7.

There are three global network parameters to be determined: the amplitude of the relaxation level oscillation ρ_0, the Q-factor of the threshold level oscillation, and the coupling coefficient d.

- The amplitude of the relaxation level oscillation ρ_0 should be a little above the crisis point so that all the BNs in the network can be in a fully chaotic state initially.
- In a preliminary numerical simulation, it turned out that the network performance as an associative memory does not depend sensitively on the choice of the Q-factor,

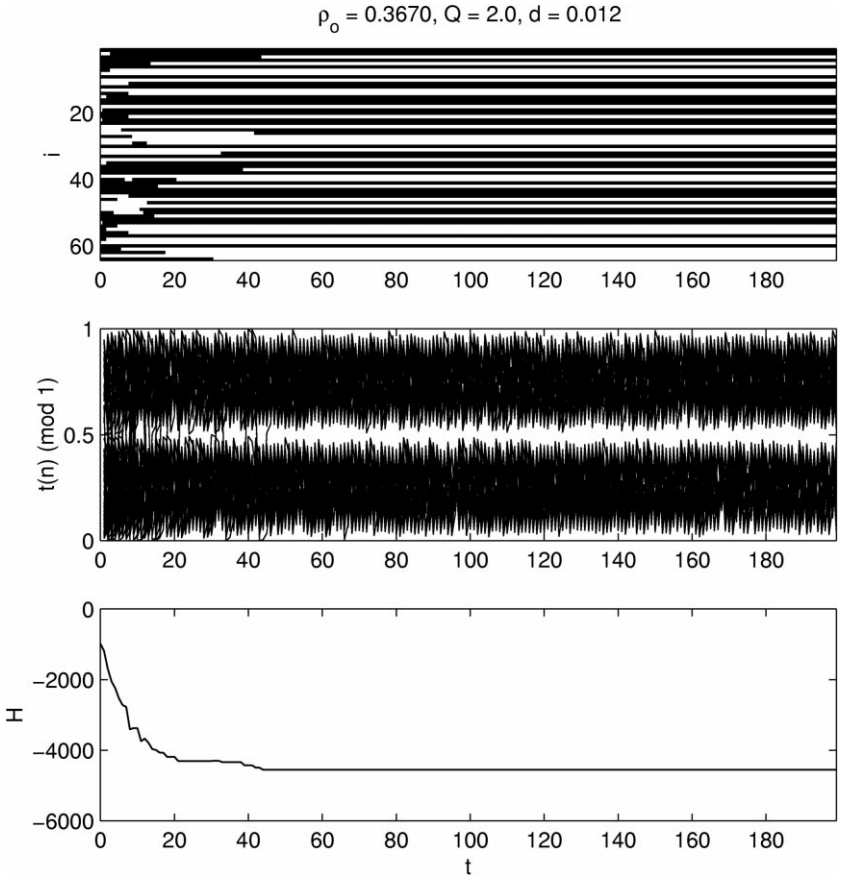

Fig. 9. The time evolution of the BNN-1 in one of the successful recall trials: (top) the transition pattern of the binary state variables $s_i(t)$; (middle) the trajectories of all the firing time series $t_i(t)$; and (bottom) the trend of the pseudo energy function H(t).

provided it is not too small. The behavior of the network was not very different for the following two cases: $Q = 2$ and $Q = 3$.

- The coupling strength d can be determined only by trial and error. If it is too small, the network can never settle to a stable pattern. On the other hand, if it is too large, the network tended to settle down too early to a spurious pattern. A preliminary simulation showed that, when $I = 64$ and $K = 6$, $d = 0.012$ was a reasonable choice.

A series of computer simulations was carried out to examine the dynamics of the BNN-1 with the following network parameters: $I = 64$; $\rho_0 = 0.367$ and 0.368; $Q = 2$, 2.5, and 3; $d = 0.01$, 0.012, and 0.014. The BNN-1 spends more time before it recalls a stored pattern compared with the Hopfield network. In fact, this is more of an advantage than a disadvantage: the network performs a more thorough search for stored patterns. This means that the BNN-1 would be less susceptible to the spurious local minima problem. We used the same associative memory test that was defined in the previous section to assess the recall quality of the BNN-1. We repeated the same test for many different values of the parameters ρ_0, Q and d, and the result is tabulated in Table 2. For almost all the combinations of the parameters, the BNN-1 appears to outperform the Hopfield network, whose test result was shown in the previous section. In particular, when $\rho_0 = 0.368$, $Q = 2.0$ and $d = 0.012$, the BNN-1 successfully recalled a stored pattern without a single exception, i.e. it was literally free from the interference of any spurious local minima.

Fig. 9 shows the time evolution of the BNN-1 in one of the successful recalls. The top plot shows the transition pattern of the binary states of all the BNs in the network. A negative state ($s(t) = -1$) is represented in black, while a positive state ($s(t) = 1$) is represented in white. It took the network about 60 unit time before it could recall a stored pattern. This plot can give the wrong impression that the network is converging to a static pattern. Of course, this is not true, and the network stays in a chaotic state throughout the whole recall process. This fact is shown clearly in the middle plot that shows the firing time series of all the BNs in the network. For an initial transient period, the BNs fire at any point in the state space, i.e. both in the n-period and in the p-period. Around $t = 20$, the BNs start to form two groups, one with BNs firing in the n-period and the other with BNs firing in the p-period. Such clusters, in fact, exactly correspond to the two groups of BNs that we pictured in Fig. 6. The stabilization of the two groups,

Table 2
The recall performance of the current network. The numbers in the table represent the number of successful recalls of the patterns specified in the column headings

ρ_0	Q	d	$\mathscr{P}_1/\overline{\mathscr{P}}_1$	$\mathscr{P}_2/\overline{\mathscr{P}}_2$	$\mathscr{P}_3/\overline{\mathscr{P}}_3$	$\mathscr{P}_4/\overline{\mathscr{P}}_4$	$\mathscr{P}_5/\overline{\mathscr{P}}_5$	$\mathscr{P}_6/\overline{\mathscr{P}}_6$	Total
0.367	2.0	0.010	57/90	160/85	117/136	71/69	14/19	68/59	945
0.367	2.0	0.012	52/69	121/85	103/117	138/150	20/22	72/39	988
0.367	2.0	0.014	42/74	124/78	105/110	152/157	28/20	57/45	992
0.367	2.5	0.010	38/68	95/51	87/105	163/173	23/30	46/32	911
0.367	2.5	0.012	40/64	104/69	82/94	156/182	30/20	42/29	912
0.367	2.5	0.014	48/67	116/64	93/104	121/139	23/19	46/43	883
0.367	3.0	0.010	34/62	102/42	87/87	124/126	28/24	41/30	787
0.367	3.0	0.012	46/64	104/48	82/91	77/86	28/19	40/31	716
0.367	3.0	0.014	39/64	106/56	93/94	23/17	26/20	38/35	611
0.368	2.0	0.010	58/102	183/116	138/159	47/35	12/8	83/50	991
0.368	2.0	0.012	55/87	152/79	110/130	114/107	21/17	73/55	1000
0.368	2.0	0.014	46/78	143/82	108/127	134/142	22/17	53/46	998
0.368	2.5	0.010	38/64	108/66	96/109	172/181	19/19	51/35	958
0.368	2.5	0.012	34/68	109/59	91/101	163/190	28/19	45/34	941
0.368	2.5	0.014	53/74	124/69	98/107	114/135	24/26	49/40	913
0.368	3.0	0.010	36/69	93/46	92/94	142/162	30.13	42/34	853
0.368	3.0	0.012	44/62	104/54	86/96	87/116	27/19	43/33	771
0.368	3.0	0.014	40/71	98/61	92/93	20/22	23/17	41/35	613

therefore, indicates the completion of a recall process. Note, however, that the network is still exhibiting chaos, though it is not full-blown, even after the recall process is completed. Comparing Figs. 8 and 9 makes it more clear what we meant to say in Fig. 2: Fig. 8 depicts a convergence to the bottom of a basin of attraction while Fig. 9 depicts a convergence to a chaotic attractor that spans almost an entire basin of attraction.

The bottom plot in Fig. 9 shows the trend of the pseudo-energy function of the BNN-1, which is defined by Eq. (17). Note that the pseudo-energy function is not always decreasing but is sometimes increasing, as if the BNN-1 is striving to get out of a spurious minimum. This behavior is in sharp contrast with that of the Hopfield network shown in Fig. 8, where the pseudo-energy function can only move down destined by the gradient descent dynamics of the Hopfield network.

Another recall process of the BNN-1 is shown in Fig. 10. In this case, the network failed to converge to any of the stored patterns. For some length of the initial period, it appears to stabilize, but can never settle down to a stable pattern. This behavior is considered to be a very useful feature of the BNN-1 since it can be interpreted as an 'I don't know' state. If the network had been following the gradient descent dynamics like the Hopfield network, it would have converged to a static pattern anyway, regardless of the validity of the convergent pattern. If a network can say 'I don't know', we can know that the initial pattern (the initial state) does not resemble any of the training patterns or the reversed patterns.

Before we conclude this section, it may be worth looking at what is going on inside the network to convince ourselves of its proper operation. Fig. 11 shows the time evolution of the internal state of the first six BNs in the network during the recall process that was depicted in Fig. 10. The left and right plots show the state of the BNs in the initial phase and in the final phase of the recall process, respectively. Notice the spontaneous development of sinusoidal oscillation on the threshold level as the recall process proceeds. Initially, the threshold level is flat or random, so the BNs have a chance to switch between the n-period and the p-period freely. As the sinusoidal oscillation develops, the BNs are forced to choose one of the two periods, and in a phase-locked manner. The phase-locking, after a recall process is complete, binds all the BNs together to maintain the recalled pattern. The whole process is autonomous, i.e. no external control of the network parameters is necessary to guide its stabilization.

7. Conclusion

We found out that the BN can exhibit bistability (in fact, multi-stability), which is controlled by attactor-merging crisis. Also, we found out the introduction of a sinusoidal perturbation in the threshold level of the BN can break the symmetry of the bistability. These findings led us to the design of the BNN-1, where each BN is operating in a chaotic mode, but can still encode a binary value. We assessed the capability of the BNN-1 as an associative memory and found out that the network would almost always converge to a stored pattern when the network parameters were properly selected. This result was in sharp contrast to the case of the Hopfield network, which suffered from spurious local minimum problem.

Before we conclude this paper, we will summarize some characteristics and attributes of the BNN-1 that distinguish

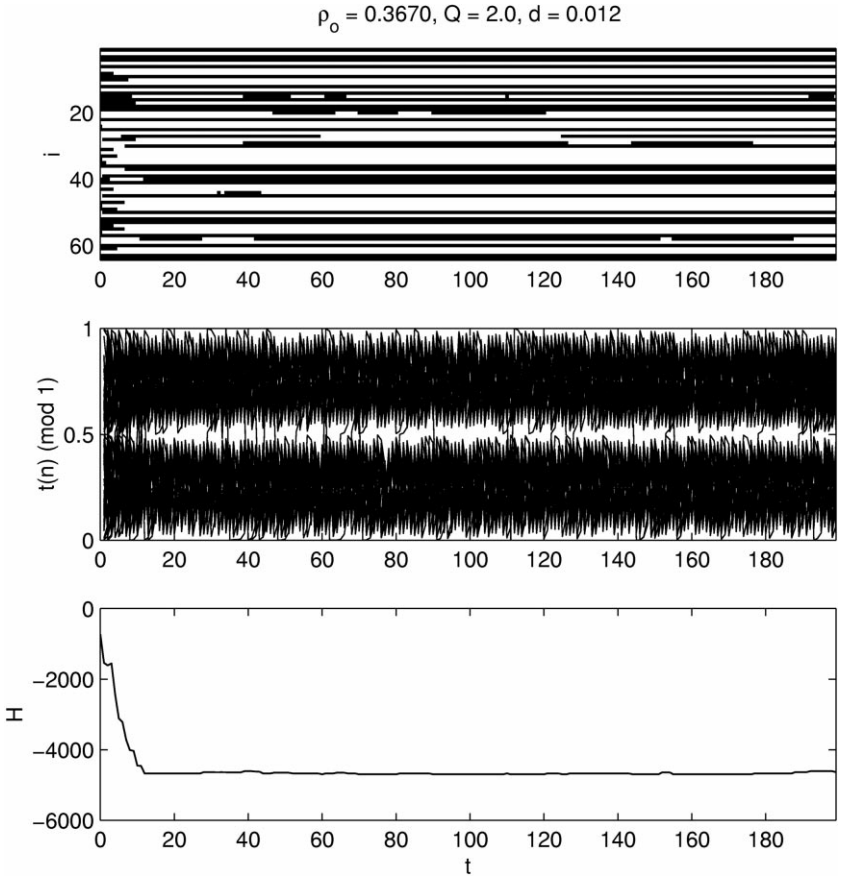

Fig. 10. The time evolution of the BNN-1 in one of the 'unsuccessful' recall trials: (top) the transition pattern of the binary state variables $s_i(t)$; (middle) the trajectories of all the firing time series $t_i(t)$; and (bottom) the trend of the pseudo energy function H(t).

it from other types of artificial neural networks.

- In the BNN-1, the average firing rate of every BN is always 1, no matter how chaotic the firing may be. This means that the BNs make use of the relative timing of the output spikes in their interaction. If we had used the average firing rate of the BN as its output, the network would have been able to produce nothing. This is in sharp contrast to the sigmoidal neural networks.
- The BNN-1 is always operating in a chaotic mode, and therefore the inter-spike intervals of the individual BNs can never be constant. Stofky & Kock (Softky & Koch, 1993) reported high variability of the inter-spike intervals in their analysis of data from the cat and the primary visual cortex (V1) and extrastriate cortex (MT) neurons. Their finding was inconsistent with the neural networks that are based on the leaky integrate-and-fire neuron model (Knight, 1972), but are, apparently, in agreement with our network.
- The chaotic activity in our network is self-organizing. Given a random initial condition, it always starts with a maximally chaotic, transient period. However, as its recall proceeds, the chaotic activity decreases gradually. After the recall process is complete, the collective activity of the network can be described as a regular series of spike bursts. This characteristic strongly reminds us of the experimental finding of Freeman (Freeman & Skarda, 1985; Freeman, 1986; Skarda & Freeman, 1987) which was described earlier.
- The self-organizing chaotic activity will be of a practical value when the BNN-1 is applied to solving an optimization problem since no external control of the degree of chaos is required. The chaotic activity decreases automatically as it approaches a stable pattern. This is not at all very common in other networks that are designed to solve optimisation problems, and many of them require a form of parameter scheduling, such as the temperature scheduling in the simulated annealing algorithm (Kirkpatrick, Gelatt, & Vecchi, 1983; Geman & Geman, 1984). The Boltzman machines (Hinton & Sejnowski, 1983; Ackley, Hinton & Sejnowski, 1985), the Gaussian machine (Akiyama, Yamashira, Kajiura, Anzai, & Aiso, 1991), gain sharpening of the Hopfield network (Hopfield & Tank, 1985), and mean field approximation annealing (Peterson & Anderson, 1987) are some examples that require a kind of parameter scheduling.
- The BNN-1 is particularly suited for circuit implementation. The oscillatory dynamics of a BN can be realized by a relaxation oscillator circuit using a simple element, such as a programmable unijunction transistor (PUT).

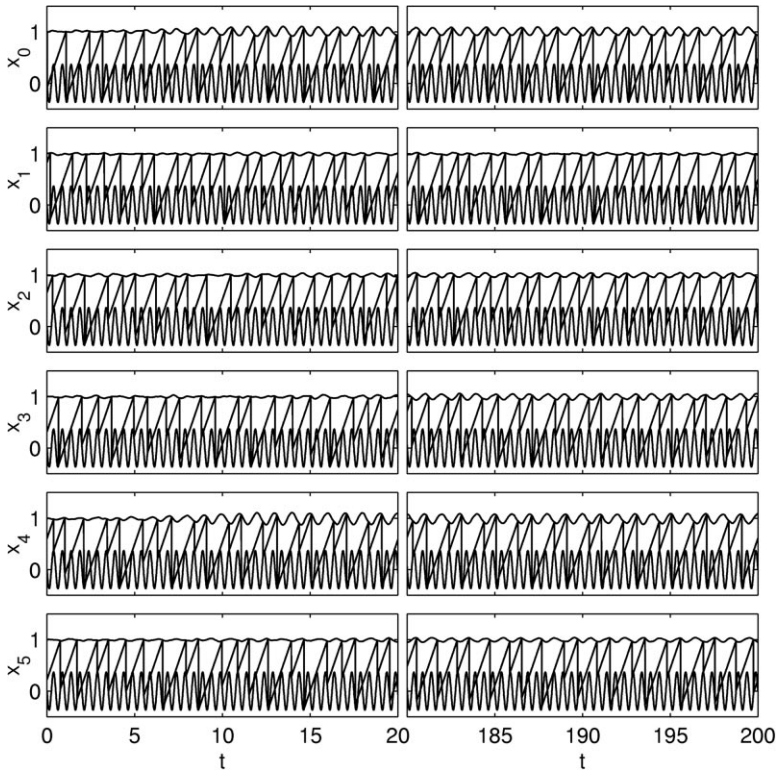

Fig. 11. The time evolution of the first six BNs in the network during the recall process shown in Fig. 9.

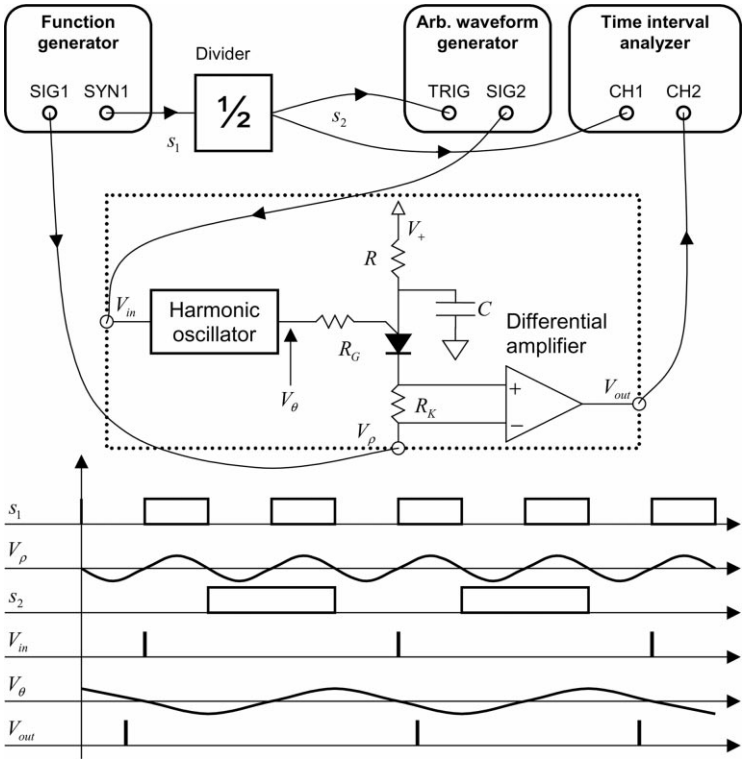

Fig. 12. The experimental setup to test one possible circuit model of the BN: a series combination of a harmonic oscillator and a relaxation oscillator. An arbitrary waveform generator is providing a spike train input to the BN, and a time interval analyzer is measuring the firing time of the BN.

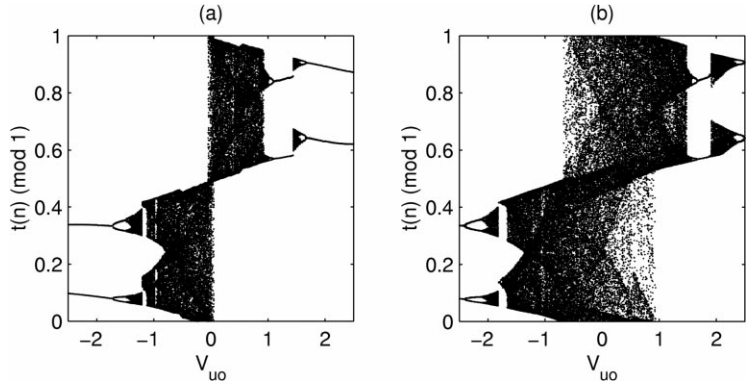

Fig. 13. The bifurcation diagrams obtained from the experimental setup shown in Fig. 12: a, when the relaxation level amplitude is near the crisis point, and b, when the relaxation level is a little above the crisis point.

Also, the response of the threshold level of a BN to an incoming spike train can be modeled by a simple RLC circuit or an active filter circuit. In addition, summing of the fanning-in spike trains does not require an analog summing amplifier. Instead, a simpler circuit, such as an OR gate circuit, will be sufficient since the spikes in the trains are spread nearly uniformly in time. The circuit implementation of the BNN-1 is one of our ongoing projects. Fig. 12 shows a preliminary experiment to test one possible circuit model of the BN: a series combination of a harmonic oscillator (a low-pass Sallen and Key filter (Chen, 1995) and a relaxation oscillator (a PUT oscillator). An arbitrary waveform generator is providing a spike train input to the BN, and a time interval analyzer is measuring the firing time of the BN. The bifurcation diagrams obtained from the experimental setup is shown in Fig. 13 where the amplitude of the input spike train is the bifurcation parameter. This experimental result shows that the simple BN circuit is clearly capable of reproducing the essential dynamical characteristics of the BN, i.e. the bistability and the attractor-merging crisis of the BN.

Acknowledgements

This research was supported by the Office of Naval Research under grant no. N00014-94-1-0931.

References

Abbott, L. F., & van Vreeswijk, C. (1993). Asynchronous states in networks of pulse-coupled oscillators. *Physical Review E*, *48* (2), 1483–1490.

Ackley, D. H., Hinton, G. E., & Sejnowski, T. J. (1985). A learning algorithm for Boltzmann machines. *Cognitive Science*, *9*, 147–169.

Adrian, E. D. (1926). The impulses produced by sensory nerve endings. *Journal of Physiology*, *61*, 49–72.

Aihara, K., & Matsumoto, G. (1986). Chaotic oscillations and bifurcations in squid giant axons. In A. V. Holden, *Chaos* Princeton University.

Aihara, K., & Takabe, T. (1990). Chaotic neural networks. *Physics Letters A*, *144* (6,7), 333–340.

Akiyama, Y., Yamashira, A., Kajiura, M., Anzai, Y., & Aiso, H. (1991). The Gaussian machine: a stochastic neural network for solving assignment problems. *Journal of Neural Network Computation*, *2*, 14–23.

Babloyantz, A., & Destexhe, A. (1986). Low-dimensional chaos in an instance of epilepsy. *Proceedings of the National Academy of Sciences of the USA*, *83*, 3513–3517.

Babloyantz, A., Nicolis, C., & Salazar, M. (1985). Evidence of chaotic dynamics of brain activity during the sleep cycle. *Physics Letters A*, *111*, 152–156.

Baek, A. S., & Farhat, N. H. (1998). Biomorphic networks: approach to invariant feature extraction and segmentation for atr. In *Radar processing, technology, and applications III* (pp. 228–239). San Diego, CA: SPIE.

Basar, E. (1983). Synergetics of neural populations, survey on experiments. In E. Basar, H. Haken & A. J. Mandell, *Synergetics of the brain* (pp. 183–200). Springer.

Bottani, S. (1995). Pulse-coupled relaxation oscillators: from biological synchronization to Self-organized Criticality. *Physical Review Letters*, *74* (21), 4189–4192.

Bressler, S. L., & Freeman, W. J. (1980). Frequency analysis of olfactory system EEG in cat, rabbit, and rat. *Electroencephalography and Clinical Neurophysiology*, *50*, 19–24.

Chen, W. -K. (1995). *The circuits and filters Handbook*, CRC Press.

Crick, F. (1984). Function of the thalamic reticular complex: the searchlight hypothesis. *Proceedings of the National Academy of Sciences of the USA*, *81* (14), 4586–4590.

Eckhorn, R., Arndt, M., & Dike, P. (1990). Feature linking via synchronization among distributed assemblies: simulation results from cat visual cortex. *Neural Computation*, *2*, 293–307.

Eckhorn, R., Bauer, R., Jordan, W., Brosch, M., Kruse, W., Munk, M., & Reitboeck, H. J. (1988). Coherent oscillations: a mechanism of feature linking in the visual cortex? *Biological Cybernetics*, *60*, 121–130.

Farhat, N. H., & Eldefrawy, M. (1991). The bifurcating neuron. In *Digest Annual OSA Meeting, San Jose, CA*.

Farhat, N. H., & Eldefrawy, M. (1992). The bifurcating neuron: characterization and dynamics. In *Photonics for computers, neural networks, and memories*, volume 1773 of *SPIE Proceedings*, (pp. 23-34. San Diego, CA: SPIE.

Farhat, N. H., & Hernandez, E. D. M. (1995). Logistic networks with DNA-like encoding and interactions. In *Lecture notes in computer science*, volume 930 (pp. 214-222). Berlin: Springer-Verlag.

Freeman, W. (1986). Petit mal seizure spikes in olfactory bulb and cortex caused by runaway inhibition after exhaustion of excitation. *Brain Research Reviews*, *11*, 259.

Freeman, W., Skarda, C. A., & Spatial, E. E. G. (1985). patterns, nonlinear

dynamics and perception: neo-Sherringtonian view. *Brain Research Reviews*, *10*, 147.

Freeman, W., & van Dijk, B. W. (1987). Spatial patterns of visual cortical fast eeg during conditioned reflex in a rhesus monkey. *Brain Research*, *422*, 267–276.

Geman, S., & Geman, D. (1984). Stochastic relaxation, Gibbs distributions, and the Bayesian restoration of images. *IEEE Transactions on Pattern Analysis and Machine Intelligence*, *6* (6), 721–741.

Gray, C. M., & Singer, W. (1989). Stimulus-specific neuronal oscillations in orientation columns of cat visual cortex. *Proceedings of the National Academy of Sciences of the USA*, *86*, 1698–1702.

Grebogi, C., Ott, E., & Yorke, J. A. (1987). Unstable periodic orbits and the dimension of chaotic attractors. *Physical Review A*, *36* (7), 3522–3524.

Hayashi, H., Ishizuka, S., Ohta, M., & Hirakawa, K. (1982). Chaotic behavior in the onchidium giant neuron under sinusoidal stimulation. *Physics Letters A*, *88* (8), 435–438.

Haykin, S. (1994). *Neural networks: a comprehensive foundation*, New York: Macmillan.

Hebb, D. O. (1949). *The organization of behavior: a neuropsychological theory*, New York: Wiley.

Hertz, J., Krogh, A., & Palmer, R. G. (1991). *Introduction to the theory of neural computation, volume 1 of Santa Fe Institute Studies in the Sciences of Complexity*, Addison-Wesley.

Hilborn, R. C. (1994). *Chaos and nonlinear dynamics, an introduction for scientists and engineers*, New York: Oxford University Press.

Hinton, G. E., & Sejnowski, T. J. (1983). Optimal perceptual inference. In *Proceedings of the IEEE Conference on Computer Vision and Pattern Recognition*, Washington, DC.

Hodgkin, A. L., & Huxley, A. F. (1952). A quantitative description of membrane current and its application to conduction and excitation in nerve. *Journal of Physiology*, *117*, 500–544.

Holden, A. V., Hyde, J., Muhamad, M. A., & Zhang, H. G. (1992). Bifurcating neuron. In J. G. Taylor, *Coupled oscillating neurons*London: Springer-Verlag.

Holden, A. V., & Ramadan, S. M. (1981). The response of a molluscan neuron to a cyclic input: entrainment and phase-locking. *Biological Cybernetics*, *41*, 157–163.

Holden, A. V., Tucker, J. V., Zhang, H., & Poole, M. J. (1992). Coupled map lattice as computational systems. *Chaos*, *2* (3), 367–376.

Hopfield, J. J. (1982). Neural networks and physical systems with emergent collective computational abilities. *Proceedings of the National Academy of Sciences of the USA*, *79*, 2554–2558.

Hopfield, J. J. (1995). Pattern recognition computation using action potential timing for stimulus representation. *Nature*, *376* (6), 33–36.

Hopfield, J. J., & Tank, D. W. (1985). Neural computation of decisions in optimization problems. *Biological Cybernetics*, *52*, 141–152.

Johnson, J. L. (1994). Pulse-coupled neural network. In Chen, S.-S., & Caulfield, H. J. (Eds.), *Adaptive computing: mathematics, electronics, and optics*, volume CR55 of Critical Reviews of Optical Science and Technology (pp. 47–76). SPIE.

Kaneko, K. (1992). Overview of coupled map lattices. *Chaos*, *2* (3), 279–282.

Kaneko, K. (1993). *Theory and applications of coupled map lattices*, John Wiley & Sons: Chichester, New York.

Kirkpatrick, S., Gelatt Jr, C. D., & Vecchi, M. P. (1983). Optimization by simulated annealing. *Science*, *220*, 4598.

Knight, B. W. (1972). Dynamics of encoding in a population of neurons. *Journal of General Physiology*, *59*, 734–766.

Krieger, D., & Dillbeck, M. (1987). High frequency scalp potentials evoked by a reaction time task. *Electroencephalography and Clinical Neurophysiology*, *67*, 222–230.

Maass, W., & Natschlaeger, T. (1998). Associative memory with networks of spiking neurons in temporal coding. In L. S. Smith & A. Hamilton, *Neuromorphic Systems: Engineering silicon from neurobiology*Singapore: World Scientific.

McKenna, T., Davis, J., & Zornetzer, S. F. (1992). *Single neuron computation*, Boston: Academic Press.

Milner, P. M. (1974). A model for visual shape recognition. *Psychology Review*, *81*, 521–535.

Mirollo, R. E., & Strogatz, S. H. (1990). Synchronization of pulse-coupled biological oscillators. *SIAM Journal on Applied Mathematics*, *50*, 1645–1662.

Natschlaeger, T., & Ruf, B. (1998). Spatial and temporal pattern analysis via spiking neurons. *Network: Computation in Neural Systems*, *9*, 319–332.

Nicolis, J. (1986). Chaotic dynamics applied to information processing. *Reports on Progress in Physics*, *49* (10), 1109–1196.

Nicolis, J. S. (1991). *Chaos and information process: a heuristic outline*, Singapore, Teaneck, NJ: World Scientific.

Nozawa, H. (1992). A neural network model as a globally coupled map and applications based on chaos. *Chaos*, *2* (3), 377–386.

O'Keefe, J., & Dostrovsky, J. (1971). The hippocampus as a spatial map: preliminary evidence from unit activity in the freely-moving rat. *Brain Research*, *34* (1), 171–175.

O'Keefe, J., & Recce, M. L. (1993). Phase relationship between hippocampal place units and the EEG theta rhythm. *Hippocampus*, *3* (3), 317–330.

Ott, E., Grebogi, C., & Yorke, J. A. (1990). Controlling chaos. *Physical Review Letters*, *64* (11), 1196–1199.

Peterson, C., & Anderson, J. R. (1987). A mean field theory algorithm for neural networks. *Complex Systems*, *1*, 995–1019.

Rabinovitch, M. I., & Abarbanel, H. D. I. (1998). The role of chaos in neural systems. *Neuroscience*, *87* (1), 5–14.

Rapp, P. E., Zimmerman, I. D., Albano, A. M., Deguzman, G. C., & Greenbaum, N. N. (1985). Dynamics of spontaneous neural activity in the simian motor cortex: the dimension of chaotic neurons. *Physics Letters A*, *110*, 335–338.

Rieke, F., Warland, D., de Ruyter van Steveninck, R., & Bialek, W. (1996). *Spikes—exploring the neural code*, Cambridge, MA: MIT Press.

Segev, L., Fleshman, J. W., & Burke, R. E. (1989). Compartment models of complex neurons. In C. Koch & I. Segev, *Methods in neuronal modelling*, Cambridge, MA: MIT Press.

Skarda, C. A., & Freeman, W. J. (1987). How brains make chaos in order to make sense of the world. *Behavioral Brain Research*, *10*, 161–195.

Softky, W. R., & Koch, C. (1993). The highly irregular firing of cortical cells is inconsistent with temporal integration of random EPSPs. *Journal of Neuroscience*, *13*, 334–350.

Sompolinsky, H., & Crisanti, A. (1988). Chaos in random neural networks. *Physical Review Letters*, *61* (3), 259–262.

von der Malsburg, C. (1981). The correlation theory of brain function. Internal Report 81-2. Gottingen: Max-Planck Institute for Biophysical Chemistry.

Wang, L., & Smith, K. (1988). On chaotic simulated annealing. *IEEE Transactions on Neural Networks*, *9* (4), 716–718.

Wheeler, D. W. (1998). Nonlinear behavior in small neural systems. PhD thesis, University of Texas, Austin, www.pitt.edu.

Yao, Y., & Freeman, W. J. (1990). Model of biological pattern recognition with spatially chaotic dynamics. *Neural Networks*, *3*, 153–170.